EurJIC European Journal of Inorganic Chemistry

ChemPubSoc Europe

SHORT COMMUNICATION

DOI:10.1002/ejic.201300099

Approaches to Molecular Magnetic Materials from the Use of Cyanate Groups in Higher Oxidation State Metal Cluster Chemistry: Mn_{14} and Mn_{16}

Dimitris I. Alexandropoulos,[a] Constantina Papatriantafyllopoulou,[b] Chaoran Li,[b] Luís Cunha-Silva,[c] Manolis J. Manos,[d] Anastasios J. Tasiopoulos,[e] Wolfgang Wernsdorfer,[f] George Christou,[b] and Theocharis C. Stamatatos*[a]

Keywords: Cluster compounds / Cyanates / Manganese / N,O ligands / Single-molecule magnets

The initial employment of cyanato groups in higher oxidation state manganese cluster chemistry, in conjunction with the gem-diolate form of di-2-pyridylketone or 2,6-diacetylpyridine dioxime chelate ligands, has afforded structurally interesting $Mn^{II/III}_{14}$ and $Mn^{II/III/IV}_{16}$ clusters, respectively. In both complexes, the end-on bridging cyanato groups show an obvious preference in binding through their O atom, a significantly different ligation than that for the homoatomic-type N_3^- ligand. The Mn_{14} compound shows entirely visible out-of-phase signals below 5 K and large hysteresis loops below 2 K.

Introduction

The fascination of inorganic chemists with manganese coordination chemistry has been primarily driven by its relevance to bioinorganic chemistry and single-molecule magnetism. Single-molecule magnets (SMMs) have a significant energy barrier to magnetization relaxation, and the upper limit to the barrier (U) is given by $S^2|D|$ or $(S^2-1/4)|D|$ for integer and half-integer spin, respectively.[1] Thus, SMMs represent a molecular route to nanoscale magnetism, with potential applications in information storage[2] and spintronics[3] at the molecular level, and use as quantum bits in quantum computation.[4]

The employment of azido groups in higher oxidation state Mn cluster chemistry has recently renewed the interest of coordination chemists and magnetochemists.[5] This was basically because of the coordination flexibility of the N_3^- ions and the ferromagnetic coupling they promote when they bridge in the 1,1-fashion (end-on). The combination of these two characteristics has led to a large number of new Mn^{III}-containing clusters with nuclearities of up to $\{Mn_{32}\}$[6] and S values as large as 83/2,[7] 74/2,[8] and 51/2.[9]

The use of OCN^- groups in *divalent* 3d-metal cluster chemistry has been extensively investigated. However, the role of OCN^- never had the impact of N_3^-, and when they were employed in M^{2+} chemistry, it was mainly for magnetostructural reasons, i.e. for comparison of the strength of the magnetic exchange interactions between *structurally similar* M^{2+}/N_3^- and M^{2+}/OCN^- complexes.[10–12] The highest nuclearity M^{2+}/OCN^- complex to date is a Fe^{II}_9 cluster,[11a] which is isomorphous with the Co^{II}_9[11b] and Ni^{II}_9[11c] analogues.

There has been little use of OCN^- in higher oxidation state metal chemistry, and particularly in Mn^{III} coordination chemistry.[8,12] Reasons for that are probably the assumed structural similarities of the many currently known Mn^{III}/N_3^- clusters with the corresponding Mn^{III}/OCN^- species,[8,12a] as well as the assumed magnetic similarities between the two families of complexes that might not lead to any new, significant magnetic results. Hendrickson and coworkers have recently reported two isostructural $Mn^{II}_2Mn^{III}_3$ clusters containing either N_3^- or OCN^- groups;[12b] the Mn_5/N_3^- compound is ferromagnetically-coupled, whereas the isostructural Mn_5/OCN^- compound exhibits an antiferromagnetic behavior. However, in the present work we show

[a] Department of Chemistry, Brock University, L2S 3A1 St. Catharines, Ontario, Canada
Fax: +1- 905-6829020
E-mail: tstamatatos@brocku.ca
Homepage: http://www.brocku.ca/node/8772
[b] Department of Chemistry, University of Florida, Gainesville, Florida 32611-7200, USA
[c] REQUIMTE & Department of Chemistry and Biochemistry, Faculty of Sciences, University of Porto, 4169-007 Porto, Portugal
[d] Department of Chemistry, University of Ioannina, 45110 Ioannina, Greece
[e] Department of Chemistry, University of Cyprus, 1678 Nicosia, Cyprus
[f] Institut Néel, CNRS, Nanoscience Department, BP 166, 380412 Grenoble Cedex 9, France

Supporting information for this article is available on the WWW under http://dx.doi.org/10.1002/ejic.201300099.

for the first time that heteroatomic-type pseudohalides, such as OCN^-, can be employed as structure-directing ligands and ferromagnetic couplers in higher oxidation state Mn cluster chemistry, which lead to molecular species with different structural motifs and physical properties than those obtained from the corresponding reactions with N_3^-.

Previously, we have shown that reaction of azide and the *gem*-diolate of di-2-pyridylketone ($dpkd^{2-}$, Figure S1) in $Mn/MeCO_2^-$ chemistry yields the dumbbell-shaped cluster $[Mn_{26}O_8(OH)_4(N_3)_{12}(O_2CMe)_6(dpkd)_{14}(DMF)_4]$,[13] while a similar reaction but with the ligand 2,6-diacetylpyridine dioxime ($dapdoH_2$, Figure S1) in place of dpk, in the absence of $MeCO_2^-$, gives $[Mn_8O_4(OH)_6(N_3)_2(dapdo)_2(dapdoH)_2(H_2O)_2]$.[14] We now report that the analogous 1:2:1:1:1 and 2:1:2:1 reactions between $Mn(ClO_4)_2/NaO_2CMe/dpk/NEt_3/NaOCN$ and $MnCl_2/dapdoH_2/NEt_3/NaOCN$ in DMF afford the new compounds $[Mn_{14}O_4(OH)_2(OCN)_6(O_2CMe)_2(dpkd)_8(DMF)_2(H_2O)_4](OH)_2$ (**1**) and $[Mn_{16}O_8(OH)_4Cl_2(OCN)_4(L)_2(dapdo)_6(DMF)_4]$ (**2**), respectively. Note that the coordinated ligand L^{3-} is the anion of an unprecedented pyridine dioximato acid (LH_3, Figure S1), most likely generated from the in situ oxidation of one of the methyl groups of $dapdoH_2$. Such organic ligand transformations,[15] as well as the presence of OH^- counterions,[16] are with precedent in Mn cluster chemistry.

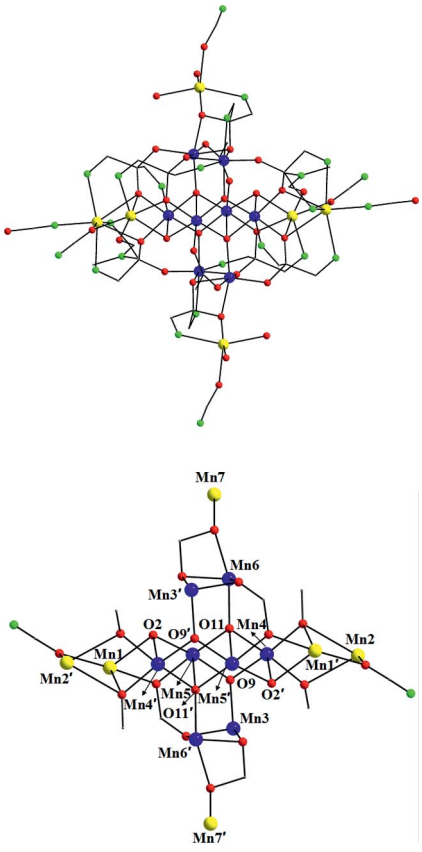

Figure 1. The structure of the cation of **1** (top) and its complete core (bottom). Only the *ipso* carbon atoms of the phenyl groups of $dpkd^{2-}$ ligands are shown. Color scheme: Mn^{II} yellow, Mn^{III} blue, O red, N green, C gray.

Results and Discussion

The cation of **1**[17] consists of a mixed-valence ($Mn^{II}_6Mn^{III}_8$) cluster (Figure 1, top), reminiscent of half of the azido-bridged $\{Mn_{26}\}$ dumbbell-shaped cluster. The Mn_{14} unit comprises a $Mn^{II}_4Mn^{III}_4$ rodlike subunit attached on either side to two symmetry-related $[Mn^{II}Mn^{III}_2(\mu\text{-}OR)_3]^{5+}$ trinuclear subunits. The 14 Mn atoms are bridged by a combination of two $\mu_4\text{-}O^{2-}$, two $\mu_3\text{-}O^{2-}$, two $\mu_3\text{-}OH^-$, two $\eta^1{:}\eta^1$ (end-on) or 2.20 (Harris notation[18]) OCN^-, and eight $dpkd^{2-}$ ligands (Scheme 1). Complex **1** thus contains an overall $[Mn_{14}(\mu_4\text{-}O)_2(\mu_3\text{-}O)_2(\mu_3\text{-}OH)_2(\mu\text{-}OCN)_2(\mu_3\text{-}OR)_2(\mu\text{-}OR)_{10}]^{12+}$ core (Figure 1, bottom), with peripheral ligation provided by two $\eta^1{:}\eta^1{:}\mu$ or 2.11 (Harris notation) $MeCO_2^-$ groups, and four OCN^-, two DMF, and four H_2O terminal ligands. Bond-valence sum (BVS) calculations[19,20] confirm the $Mn^{II}_6Mn^{III}_8$ mixed-valent description for **1**, where Mn(1,2,7) are the Mn^{II} atoms. All octahedral Mn^{III} atoms, Mn(3,4,5,6), exhibit Jahn–Teller (JT) axial elongations; the eight JT axes are essentially parallel to each other.[19] Mn2 and Mn7 are seven- and five-coordinate with distorted pentagonal-bipyramidal and square-pyramidal geometries (τ = 0.05),[21] while Mn1 is six-coordinate with a distorted octahedral geometry.

The structure of **2**[17] consists of a mixed-valence ($Mn^{II}_8Mn^{III}_4Mn^{IV}_4$) cage (Figure 2, top) with a "tubular"-like topology. The six $\mu_4\text{-}O^{2-}$, two $\mu_3\text{-}O^{2-}$, four $\mu_3\text{-}OH^-$, and four $\eta^1{:}\eta^1$ (end-on) or 2.20[18] OCN^- hold the core together, as well as six $\eta^1{:}\eta^1{:}\eta^1{:}\eta^1{:}\eta^1{:}\mu$ (or 3.11111[18]) and two $\eta^1{:}\eta^1{:}\eta^1{:}\eta^1{:}\eta^1{:}\eta^1{:}\mu$ (or 3.1110111[18]) chelating/bridging $dapdo^{2-}$ and L^{3-} groups, respectively (Scheme 1). Peripheral ligation about the core is further provided by two monodentate Cl^- atoms and four terminal DMF molecules. The core of **2** can be conveniently dissected into seven layers of four types with an ABCDCBA arrangement (Figure 2, bottom): Mn^{II} monomeric layer A is the "lid" (or "base") of the Mn_{16} "tube", linked to layer B, which has an unusual oxidation state description, $Mn^{II}_2Mn^{III}Mn^{IV}$ "butterfly"; layer C is a "node"-like Mn^{III} monomer, which acts as the connector between layers AB and D; the latter, central layer D is again a "butterfly"-type unit but with a $Mn^{II}_2Mn^{IV}_2$ description. Each layer is held together and linked to neighboring layers by a combination of oxido, alkoxido, oximato, and end-on cyanato ligands.

In both **1** and **2**, the end-on bridging cyanato groups show an obvious preference in binding through their O atom (hard donor atom), a significantly different ligation than that for the homoatomic-type N_3^- ligand. Indeed, **1** and **2** are the first OCN^--based clusters in which the metal centers are O-bridged, which opens a new window in structural 3d-metal cluster chemistry.

Solid-state dc (direct current) magnetic susceptibility (χ_M) data were collected on **1**·DMF and **2** in a 1 kG (0.1 T) field in the 5.0–300 K range. The data are plotted as $\chi_M T$ vs. T in Figure S4, and both **1**·DMF and **2** clearly have relatively large ground-state spin (S) values. The $\chi_M T$ value

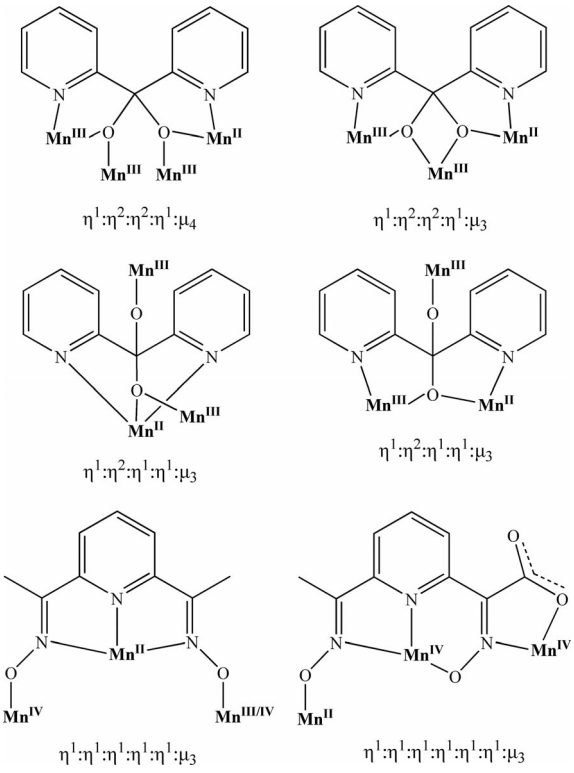

Scheme 1. The coordination modes of $dpkd^{2-}$ (top and middle), and $dapdo^{2-}$ (bottom left) and L^{3-} (bottom right) in complexes **1** and **2**.

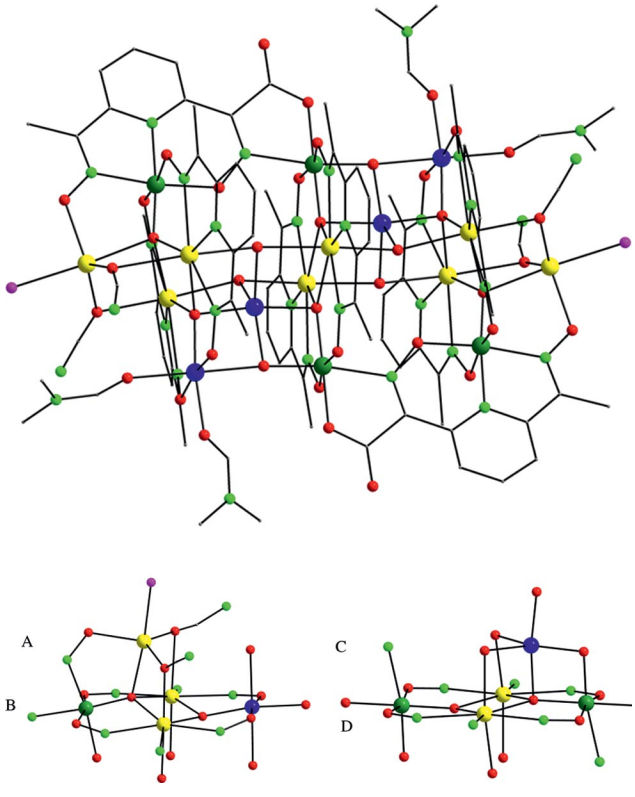

Figure 2. Structure of **2** (top) and the four types of constituent layers of its core (bottom). Color scheme: Mn^{II} yellow, Mn^{III} blue, Mn^{IV} olive, O red, N green, Cl purple, C gray.

for **1**·DMF decreases from 38.71 $cm^3\,K\,mol^{-1}$ at 300 K to 26.65 $cm^3\,K\,mol^{-1}$ at 20.0 K, and then increases to 36.73 $cm^3\,K\,mol^{-1}$ at 5.0 K. For **2**, $\chi_M T$ steadily decreases from 30.94 $cm^3\,K\,mol^{-1}$ at 300 K to a minimum of 22.39 $cm^3\,K\,mol^{-1}$ at 35.0 K, and then increases sharply to 25.61 $cm^3\,K\,mol^{-1}$ at 6.5 K, before slightly dropping to 25.50 $cm^3\,K\,mol^{-1}$ at 5.0 K. The shape of both curves suggests that both antiferro- and ferromagnetic exchange interactions are likely present within **1**·DMF and **2**.

Attempted fits of the magnetization data collected at various fields and at low temperatures, and assuming that only the ground state is populated, were poor, which suggests population of low-lying excited states, as expected for such high-nuclearity complexes. As described elsewhere,[13–16] an alternative determination of S can be reached from ac (alternating current) susceptibility measurements; this precludes complications from a dc field and/or low-lying excited states. For **1**·DMF and **2**, the in-phase (χ_M') ac signals, shown as $\chi_M' T$ in Figures 3 and S5, respectively, are very temperature dependent in the 4–15 K region, which confirms the conclusion from the dc studies of low-lying excited states. Extrapolation of the data above 15 K down to 4 K gives ≈44 and 24 $cm^3\,K\,mol^{-1}$ for **1**·DMF and **2**, which indicates S = 9 and 7 ground states, respectively (with a g value slightly less than 2). At lower temperatures, only **1**·DMF displays a frequency-dependent decrease in $\chi_M' T$ and concomitant appearance of entirely visible out-

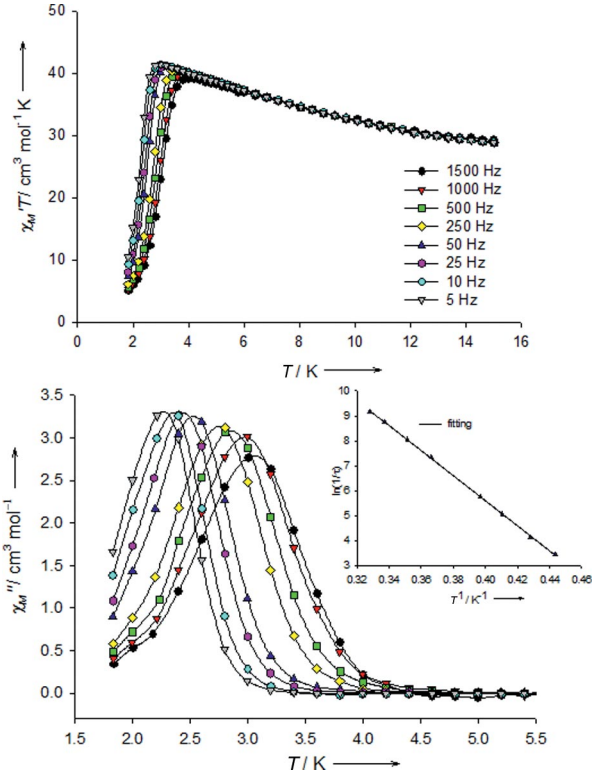

Figure 3. Plot of the in-phase (χ_M') and out-of-phase (χ_M'') ac susceptibility signals of complex **1**·DMF at the indicated frequencies. Inset: Arrhenius plot of maxima observed in χ_M''; the solid line is the fit of the thermally-activated region to the Arrhenius equation.

of-phase χ_M'' signals (Figure 3, bottom), a very rare situation for a high-nuclearity $Mn^{II/III}$ cluster and indicative of a significant barrier to magnetization relaxation. Indeed, an Arrhenius plot constructed from the ac χ_M'' vs. T data of Figure 3 (inset) gave $U_{eff} = 35$ K and $\tau_0 = 7.4 \times 10^{-12}$ s, where τ_0 is the pre-exponential factor. A U_{eff} value of 35 K is one of the highest observed for a $Mn^{II/III}$ mixed-valent complex,[13,22] still smaller than those for the Mn_6[23] and Mn_{12}[24] complexes.

The confirmation of SMM behavior for **1** was sought by magnetization vs. dc field scans on a single crystal of **1**·solv by using an array of micro-SQUIDs. These scans exhibited magnetization hysteresis loops below 2 K. The loops exhibit coercivities that increase with decreasing temperature (Figure 4) and increasing field sweep rate, but do not show the steps characteristic of quantum tunneling of magnetization as a result of step-broadening effects from low-lying excited states and distributions of local environments owing to solvent disorder.[8,9,16]

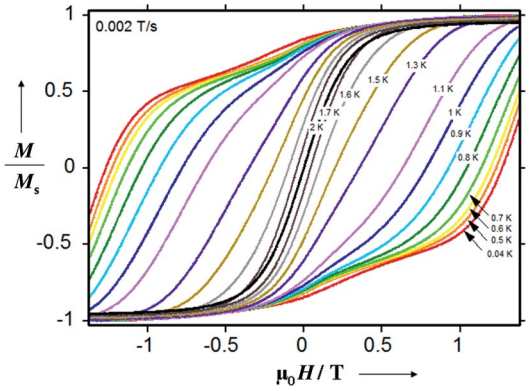

Figure 4. Magnetization (M) vs. applied dc field (H) hysteresis loops for single crystals of **1**·solv at the indicated temperatures. The magnetization is normalized to its saturation value (M_s).

Conclusions

We have reported the first results from the use of cyanato groups in higher oxidation state metal cluster chemistry, which clearly support our initial hypothesis that this area of research will lead to chemically, structurally, and magnetically new findings, distinctly different than those observed from the use of the consanguineous azido ligands.

Experimental Section

Synthesis of 1: Solid $Mn(ClO_4)_2 \cdot 6H_2O$ (0.36 g, 1.0 mmol), $NaO_2CMe \cdot 3H_2O$ (0.27 g, 2.0 mmol), and NaOCN (0.07 g, 1.0 mmol) were added to a stirred, pale yellow solution of dpk (0.18 g, 1.0 mmol) and NEt_3 (0.14 mL, 1.0 mmol) in MeCN/DMF (25 mL, 4:1 v/v). The resulting orange solution was stirred for 24 h, during which time all the solids dissolved and the color of the solution changed to dark brown. The solution was filtered, and the filtrate was left undisturbed at ambient temperature. After 10 d, X-ray quality dark red plate-like crystals of **1**·xDMF·$y$$H_2O$ appeared and were collected by filtration, washed with MeCN (2× 5 mL) and Et_2O (4× 5 mL), and dried under vacuum. Yield: 60% (0.13 g). $C_{107}H_{103}Mn_{14}N_{25}O_{41}$ (**1**·DMF): calcd. C 40.62, H 3.28, N 11.07; found C 40.60, H 3.25, N 11.38. Selected IR data (KBr): $\tilde{\nu}$ = 3442 (mb), 2180 (vs), 1656 (s), 1598 (s), 1570 (m), 1474 (w), 1436 (s), 1298 (w), 1214 (m), 1150 (m), 1116 (m), 1076 (m), 1044 (m), 1016 (s), 958 (w), 822 (w), 780 (m), 758 (m), 680 (m), 654 (m), 636 (s), 554 (m), 414 (w) cm^{-1}.

Synthesis of 2: Solid $MnCl_2 \cdot 4H_2O$ (0.20 g, 1.0 mmol) and NaOCN (0.03 g, 0.5 mmol) were added to a stirred, pale yellow solution of $dapdoH_2$ (0.10 g, 0.5 mmol) and NEt_3 (0.14 mL, 1.0 mmol) in MeCN/DMF (25 mL, 4:1 v/v). The resulting red solution was stirred for 45 min, during which time all the solids dissolved and the color of the solution changed to dark brown. The solution was filtered, and the filtrate was left undisturbed at ambient temperature. After 3 d, X-ray quality, dark brown prismatic crystals of **2**·x(solv) appeared and were collected by filtration, washed with MeCN (2× 5 mL) and Et_2O (4× 5 mL), and dried under vacuum. Yield: 45% (0.09 g). $C_{88}H_{98}Mn_{16}Cl_2N_{32}O_{40}$ (**2**): calcd. C 33.09, H 3.09, N 14.03; found C 32.79, H 3.14, N 13.86. Selected IR data (KBr): $\tilde{\nu}$ = 3440 (mb), 2182 (vs), 1654 (m), 1594 (s), 1534 (m), 1450 (m), 1390 (s), 1268 (w), 1166 (w), 1128 (m), 1050 (vs), 802 (m), 742 (w), 690 (m), 668 (mb), 624 (m), 564 (m), 484 (m), 425 (w) cm^{-1}.

Safety Note: Perchlorate salts are potentially explosive; such compounds should be synthesized and used in small quantities, and treated with utmost care at all times.

Supporting Information (see footnote on the first page of this article): Various structural and magnetism figures for complexes **1** and **2** are presented.

Acknowledgments

This work was supported by the Ontario Trillium Scholarship (to D. I. A., Th. C. S.), the Fundação para a Ciência e a Tecnologia (Pest-C/EQB/LA0006/2011 to L. C.-S.), the Cyprus Research Promotion Foundation Grant "ΑΝΑΒΑΘΜΙΣΗ/ΠΑΓΙΟ/0308/12" (to A. J. T.), the ERC Advanced Grant MolNanoSpin No. 226558 (to W. W.), and the National Science Foundation (Grant DMR-1213030 to G. C.).

[1] D. Gatteschi, R. Sessoli, *Angew. Chem.* **2003**, *115*, 278; *Angew. Chem. Int. Ed.* **2003**, *42*, 268–297.
[2] M. del Carmen Gimenez-Lopez, F. Moro, A. La Torre, C. J. Gomez-Garcia, P. D. Brown, J. van Slageren, A. N. Khlobystov, *Nat. Commun.* **2011**, *2*, 407.
[3] R. Vincent, S. Klyatskaya, M. Ruben, W. Wernsdorfer, F. Balestro, *Nature* **2012**, *488*, 357–360.
[4] G. Aromí, D. Aguilà, P. Gamez, F. Luis, O. Roubeau, *Chem. Soc. Rev.* **2012**, *41*, 537–546.
[5] a) T. C. Stamatatos, G. Christou, *Inorg. Chem.* **2009**, *48*, 3308–3322; b) A. Escuer, G. Aromí, *Eur. J. Inorg. Chem.* **2006**, 4721–4736.
[6] R. T. W. Scott, S. Parsons, M. Murugesu, W. Wernsdorfer, G. Christou, E. K. Brechin, *Angew. Chem.* **2005**, *117*, 6698; *Angew. Chem. Int. Ed.* **2005**, *44*, 6540–6543.
[7] A. M. Ako, I. J. Hewitt, V. Mereacre, R. Clérac, W. Wernsdorfer, C. E. Anson, A. K. Powell, *Angew. Chem.* **2006**, *118*, 5048; *Angew. Chem. Int. Ed.* **2006**, *45*, 4926–4929.
[8] E. E. Moushi, Th. C. Stamatatos, W. Wernsdorfer, V. Nastopoulos, G. Christou, A. J. Tasiopoulos, *Inorg. Chem.* **2009**, *48*, 5049–5051.
[9] M. Murugesu, M. Habrych, W. Wernsdorfer, K. A. Abboud, G. Christou, *J. Am. Chem. Soc.* **2004**, *126*, 4766–4767.
[10] X.-Y. Wang, Z.-M. Wang, S. Gao, *Chem. Commun.* **2008**, 281–294.

[11] a) A. K. Boudalis, B. Donnadieu, V. Nastopoulos, J. M. Clemente-Juan, A. Mari, Y. Sanakis, J.-P. Tuchagues, S. P. Perlepes, *Angew. Chem.* **2004**, *116*, 4002; *Angew. Chem. Int. Ed.* **2004**, *43*, 3912–3914; b) G. S. Papaefstathiou, S. P. Perlepes, A. Escuer, R. Vicente, M. Font-Bardia, X. Solans, *Angew. Chem.* **2001**, *113*, 908; *Angew. Chem. Int. Ed.* **2001**, *40*, 884–886; c) G. S. Papaefstathiou, A. Escuer, R. Vicente, M. Font-Bardia, X. Solans, S. P. Perlepes, *Chem. Commun.* **2001**, 2414–2415.
[12] a) S. M. J. Aubin, M. W. Wemple, D. M. Adams, H.-L. Tsai, G. Christou, D. N. Hendrickson, *J. Am. Chem. Soc.* **1996**, *118*, 7746–7754; b) P. L. Feng, C. J. Stephenson, A. Amjad, G. Ogawa, E. del Barco, D. N. Hendrickson, *Inorg. Chem.* **2010**, *49*, 1304–1306.
[13] T. C. Stamatatos, K. A. Abboud, W. Wernsdorfer, G. Christou, *Angew. Chem.* **2008**, *120*, 6796; *Angew. Chem. Int. Ed.* **2008**, *47*, 6694–6698.
[14] T. C. Stamatatos, B. S. Luisi, B. Moulton, G. Christou, *Inorg. Chem.* **2008**, *47*, 1134–1144.
[15] T. C. Stamatatos, D. Foguet-Albiol, W. Wernsdorfer, K. A. Abboud, G. Christou, *Chem. Commun.* **2011**, *47*, 274–276.
[16] a) E. Moushi, C. Lampropoulos, W. Wernsdorfer, V. Nastopoulos, G. Christou, A. J. Tasiopoulos, *J. Am. Chem. Soc.* **2010**, *132*, 16146–16155; b) T. C. Stamatatos, V. Nastopoulos, A. J. Tasiopoulos, E. Moushi, W. Wernsdorfer, G. Christou, S. P. Perlepes, *Inorg. Chem.* **2008**, *47*, 10081–10089, and references therein.
[17] a) Crystal structure data for **1**·*x*DMF·*y*H_2O: $C_{208}H_{162}Mn_{28}N_{48}O_{88}$, M_r = 6280.19, triclinic, space group $P\bar{1}$, a = 16.1201(8) Å, b = 20.8879(6) Å, c = 22.0475(10) Å, α = 85.219(3)°, β = 70.039(4)°, γ = 82.447(3)°, V = 6911.3(5) Å^3, Z = 1, $\rho_{calcd.}$ = 1.509 g cm^{-3}, T = 100(2) K, 86184 reflections collected, 23965 unique (R_{int} = 0.1368), $R1$ = 0.0694 and $wR2$ = 0.1489, using 7224 reflections with $I > 2\sigma(I)$. The small size and weak diffraction of several mounted crystals did not allow us to determine the exact number of lattice solvate molecules, a problem that is usually observed in many high-nuclearity metal complexes.[13,15,16] Crystal structure data for **2**·*x*(solv): $C_{88}H_{98}Mn_{16}Cl_2N_{32}O_{40}$, M_r = 3193.92, monoclinic, space group $P2_1/c$, a = 14.5921(4) Å, b = 21.4515(6) Å, c = 23.1946(6) Å, β = 100.600(2)°, V = 7136.5(3) Å^3, Z = 2, $\rho_{calcd.}$ = 1.486 g cm^{-3}, T = 150(2) K, 101693 reflections collected, 13532 unique (R_{int} = 0.0427), $R1$ = 0.0537 and $wR2$ = 0.1645, using 13532 reflections with $I > 2\sigma(I)$. The spaces created by the crystal packing of complexes contained considerable electron density, mainly because of disordered lattice solvate molecules (most likely DMF). Several attempts to locate and model such molecules revealed to be unsuccessful as the electron density was highly smeared-out, thus avoiding full convergence upon full-matrix least-squares refinement cycles on F^2. The searches for the total potential solvent area by using the software package PLATON[25a] revealed the existence of a large cavity with a potential solvent accessible void volume of ca. 1768 Å^3. Subsequently, the original data set was treated by using the SQUEEZE[25b] subroutines to fully remove the contribution of these highly disordered molecules in the solvent-accessible volume (contribution of ca. 988 electrons was effectively removed). The calculated solvent-free reflection list was then used for the final structure refinement; b) CCDC-905468 and CCDC-905469 contain the supplementary crystallographic data for this paper. These data can be obtained free of charge from The Cambridge Crystallographic Data Centre via www.ccdc.cam.ac.uk/conts/retrieving.html.
[18] Harris notation describes the binding mode as $X.Y_1Y_2Y_3\cdots Y_n$, where X is the overall number of metals bound by the whole ligand, and each value of Y refers to the number of metal ions attached to the different donor atoms. The ordering of Y is listed by the Cahn–Ingold–Prelog priority rules, hence here O before N. See: R. Coxall, S. G. Harris, D. K. Henderson, S. Parsons, P. A. Tasker, R. E. P. Winpenny, *J. Chem. Soc., Dalton Trans.* **2000**, 2349–2356.
[19] See the Supporting Information.
[20] a) W. Liu, H. H. Thorp, *Inorg. Chem.* **1993**, *32*, 4102–4105; b) I. D. Brown, D. Altermatt, *Acta Crystallogr., Sect. B* **1985**, *41*, 244–247.
[21] A. W. Addison, T. N. Rao, J. Reedijk, J. Rijn, G. C. Verschoor, *J. Chem. Soc., Dalton Trans.* **1984**, 1349–1356.
[22] S. Maheswaran, G. Chastanet, S. J. Teat, T. Mallah, R. Sessoli, W. Wernsdorfer, R. E. P. Winpenny, *Angew. Chem.* **2005**, *117*, 5172; *Angew. Chem. Int. Ed.* **2005**, *44*, 5044–5048.
[23] C. J. Milios, A. Vinslava, W. Wernsdorfer, S. Moggach, S. Parsons, S. P. Perlepes, G. Christou, E. K. Brechin, *J. Am. Chem. Soc.* **2007**, *129*, 2754–2755.
[24] N. E. Chakov, J. Lawrence, A. G. Harter, S. O. Hill, N. S. Dalal, W. Wernsdorfer, K. A. Abboud, G. Christou, *J. Am. Chem. Soc.* **2006**, *128*, 6975–6989.
[25] a) PLATON, A. L. Spek, *J. Appl. Crystallogr.* **2003**, *36*, 7–13; b) P. van der Sluis, A. L. Spek, *Acta Crystallogr., Sect. A* **1990**, *46*, 194–201.

Received: January 23, 2013
Published Online: March 21, 2013

